Dark current reduction with all-semiconductors nanostructured type-II superlattice LWIR photodetector

Clement Gureghian, Grégory Vincent, Jean-Baptiste Rodriguez, Guilherme Sombrio, Fernando Gonzalez-Posada, Isabelle Ribet-Mohamed, Thierrry Taliercio

Dark current reduction with all-semiconductors nanostructured Type-II superlattice LWIR photodetector

Clement Gureghian[a], Grégory Vincent[a], Jean-Baptiste Rodriguez[b], Guilherme Sombrio[b], Fernando Gonzalez-Posada[b], Isabelle Ribet-Mohamed[a], and Thierrry Taliercio[b]

[a]ONERA, 6 Chem. de la Vauve aux Granges, Palaiseau, France
[b]IES, Univ. Montpellier, CNRS, France

ABSTRACT

Achieving higher operating temperatures is a key-point in the current infrared photodetection research. One promising way to achieve this goal is through the reduction of the thickness of the active region and the use of optical resonators to compensate the consequent loss of absorption. Herein we present simulation results of the absorption in a thin LWIR T2SL photodetector, capped with heavily doped semiconductors nanostructures and the benches used to measure their properties.

Keywords: Type II superlattice, all-semiconductor, LWIR, Heavily doped semiconductors, Nanostructured detector, Thin detector, Dark current, Angular tolerance

1. INTRODUCTION

High-performance infrared photodetectors suffer from a major drawback: due to the low band-gap of the semiconductor, thermal energy is sufficient to generate electron-holes pairs at room temperature. The resulting dark-current is associated with both the noise and the detector's dynamic limit [1]. Therefore, they are cooled down to unpractical cryogenic temperatures, typically lower than 90 K for Long-Wave InfraRed (LWIR) focal plan arrays. This requires the use of cryocoolers, which are not compatible with the "Size Weight And Power" requirements and may be another cause of malfunction. Compatible with Type-II SuperLattice (T2SL) technologies, a few strategies can be investigated to lower the dark current or to allow higher operating temperatures, for instance the use of gallium-free structures or of "bariode" designs [2]. We propose here another strategy, relying on the reduction of the T2SL thickness. However, thinning of the photodetector leads to an absorption decrease. However this absorption decrease can be counterbalanced by the addition of nanostructures showing optical resonances [3]. Nanostructures are already employed in such way: for photovoltaics in order to reduce the quantity of absorber material [4] or for SWIR (short-wave infrared) applications to mitigate the short diffusion length of the free carriers colloidal nanocrystals [5]. These nanostructures are often made of metal (Ag or Au) which requires additional deposition processes. As shown in [6], heavily doped semiconductors (HDSC) are of great interest to replace them thanks to the enhanced integration capabilities offered through monolithic epitaxial growth. This use of heavily doped semiconductors has been demonstrated for structures sustaining one resonance in the LWIR and MWIR range [7,8].

In this proceeding, we focus on a LWIR multi-resonant component made out of heavily doped nanostructured InAsSb, for which we present electromagnetic computations and optical measurement methods.

Further author information: (Send correspondence to G.V.)
G.V.: E-mail: gregory.vincent@onera.fr, Telephone: +33 (0)1 80 38 63 91

2. DEVELOPED STRUCTURE

A schematic of the structure we developed is shown figure 1. It is based on a InAs/GaSb T2SL grown between a mirror and a periodically nanostructured layer. Both the mirror and the grating are made of heavily Silicon-doped InAsSb. This material has been chosen because its optical properties are similar to those of metals in the LWIR range.

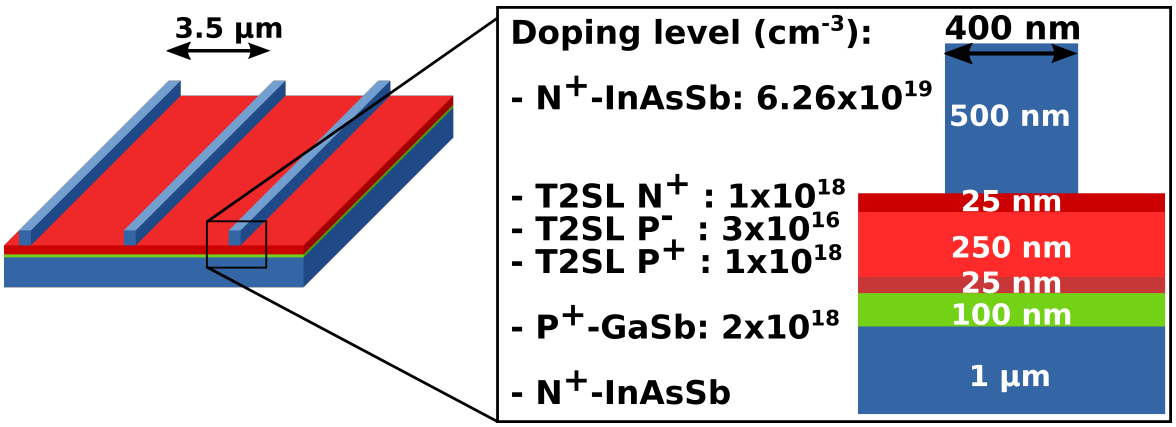

Figure 1. Representation of a multi-resonant structure for LWIR (left) and a zoom on its internal structure (right); in blue heavily doped InAsSb (bottom and top layer have the same doping level), T2SL in red and GaSb buffer zone in green.

2.1 Materials and Technology

The detector itself is a PIN photodiode of reduced thickness (300 nm instead of a few microns for a conventional detector). It is grown on a mirror-like and capped with nanostructures, both made of HDSC.

The heavily doped semiconductor used is Si-doped $InAs_{0.91}Sb_{0.09}$ at 6.26x10^{19} cm^{-3}. At this doping level, the bottom InAsSb layer acts like a mirror for LWIR and its permittivity can be described by a Drude model as [6,9]:

$$\epsilon(\omega) = \epsilon_\infty \left(1 - \frac{\omega_p^2}{\omega(\omega + i\gamma)}\right).$$

where ϵ_∞ is the high frequency permittivity of the material, γ is the damping factor, and ω_p is the screaned plasma frequency. This frequency corresponds to the limit under which the real part of the dielectric permittivity becomes negative revealing a metallic behavior of the material. The variation of the screaned plasma frequency with respect to the doping level is given by:

$$\omega_p = \frac{2\pi c}{\lambda_p} = \sqrt{\frac{Ne^2}{\epsilon_0 \epsilon_\infty m^*}}.$$

where c is the speed of light, λ_p is the plasma wavelength, N is the density of electrons, e is the electron charge, ϵ_0 is the permittivity in vacuum, ϵ_∞ the high-frequency permittivity, and m^* is the effective mass of electrons [10]. For instance, Si-doped $InAs_{0.91}Sb_{0.09}$ doped at 6.26x10^{19} cm^{-3} is expected to have a plasma frequency λ_p=5 μm.

2.2 Simulation and Design

Optical computations were performed using a RCWA library [11] to study this design. Figure 2 shows the computed absorption spectra of the structure and the different resonances within the spectral response. In this computation incident light is polarized in TM mode: magnetic field parallel to the ribbons of the grating.

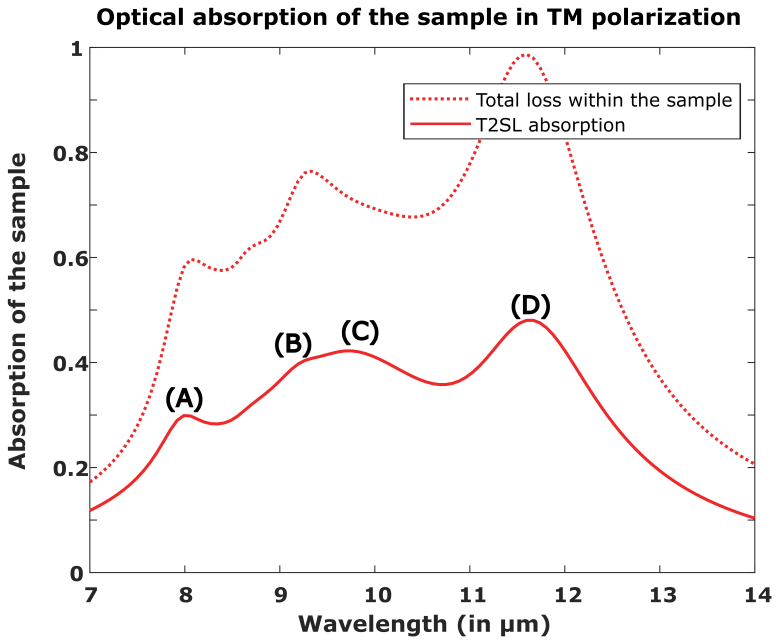

Figure 2. Spectral response of the structure at normal incidence in TM mode. The structure displays multiple resonances labeled (A) at 8 µm, (B) at 9.2 µm, (C) at 9.8 µm and (D) at 11.65 µm.

2.2.1 Light absorption within the structure

The multi-resonant approach enables a mean absorption in the T2SL layer of above 35% for the whole 8-12 μm window. This high absorption performance for our nanostructured 300 nm thick detector is comparable with that of a 2.5 μm thick bare T2SL [12]. It is achieved thanks to the four different modes participating in the absorption. Figure 3 shows the normalized dissipation maps for each of these modes. These dissipation maps allowed us to verify in which part of the detector took place the major part of the absorption. thanks to it the exact stacking of the PIN photodiode was designed.

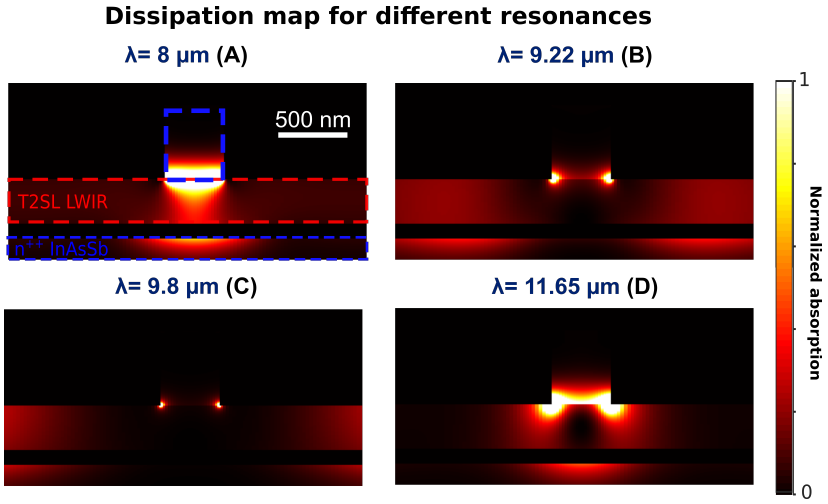

Figure 3. Normalized dissipation maps showing the distribution of absorbed incident energy for the four aforementioned resonances. Overlayed to the representation of resonance A) are the principal parts of the structure, shown in dashed lines. T2SL in red, HDSC in blue.

2.2.2 Angular properties

Each of the resonance is quite stable with respect to a varying angle of incidence. As Figure 4 shows the spectral response is stable up to 50°. This wide acceptance angle is of particular interest in potential use with convergent optics and is one of the key points during the characterization phase.

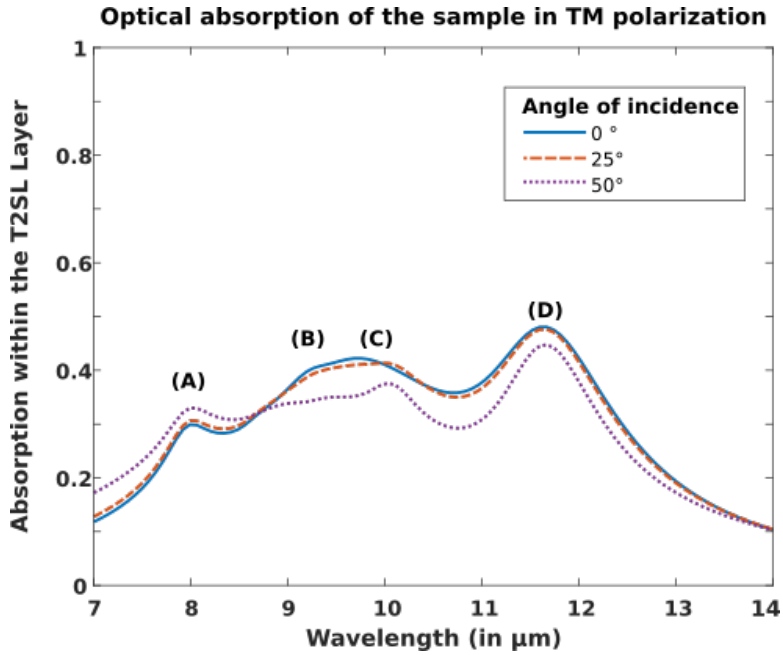

Figure 4. Computation of the absorption of the T2SL layer for TM illumination at three angles of incidence: 0°, 25° and 50°.

3. BENCHES AND MEASUREMENTS

In order to measure the expected characteristics, different benches are used. In this section we will briefly explain how measurements are carried out.

3.1 Dark Current and Spectral Response

The first bench is a circulation cryostat used to determine dark current and spectral response of the detector. Spectral response is a two step measurement. Figure 5 shows the two configurations of the cryostat during this measurement. The detector is firstly put in a cryostat in front of a Fourier Transform InfraRed (FTIR) spectrometer. The detectors field of view is limited by a cold shield at the same temperature as itself and therefore only sees the modulated signal of the FTIR through a ZnSe window of known transmission. This step enables the measurement of an unscaled, relative spectral response. The second step consists in putting the same cryostat in front of a blackbody and adding a narrow bandpass IR filter in the cold shield. Thanks to the blackbody radiation model, by varying the blackbody temperature, it is possible to rescale the spectral response and access the external quantum efficiency.

Dark current is measured by closing the cold shield with a metal lid so that the detector is fully enclosed in a cold environment and measuring the electric characteristic of the photodiode thanks to lab instrumentation. For each measurement, the output current of the photodiode is amplified and converted into tension by a transimpedance amplifier (TIA) before being digitized by an analog-to-digital converter (ADC).

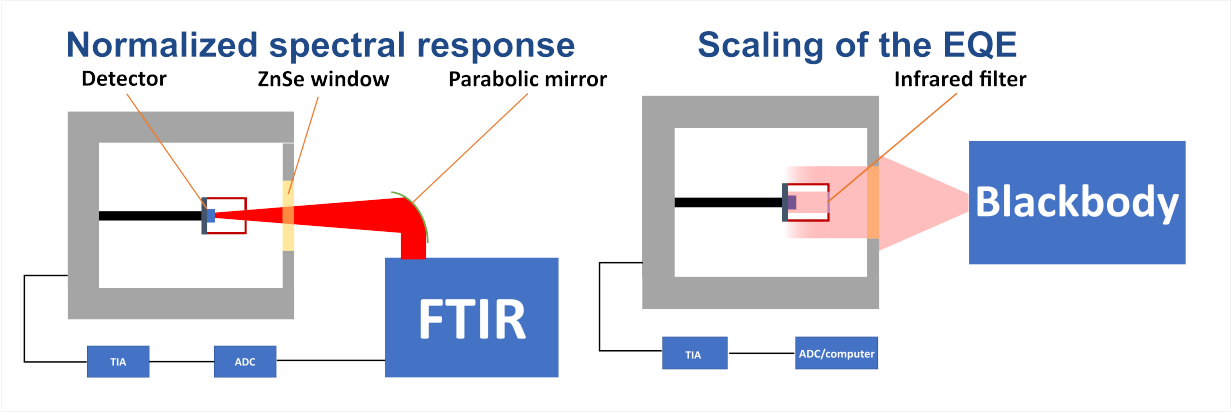

Figure 5. Schematic of the different configurations of the spectral response bench using a transimpedance amplifier and an analog-to-digital converter.

This setup enable the measurement of both dark current and external quantum efficiency. These are important metrics but other characteristics such as the specific angular response are also key features of the nanostructured photodetectors.

3.2 Angular Response

Angular response is measured thanks to a separate bench (figure 6). This one consists of a large cryostat with a vacuum sealed chamber and a small blackbody which can be rotated around the detector. A chopper is placed between the blackbody and the detector to subtract background signal due to the cryostat body at room-temperature. In addition, an IR filter can be placed in the blackbody assembly to restrict detectors illumination to a specific window. By varying the angle θ at which the detector sees the source and measuring its output, one can access the relative angular response of the detector.

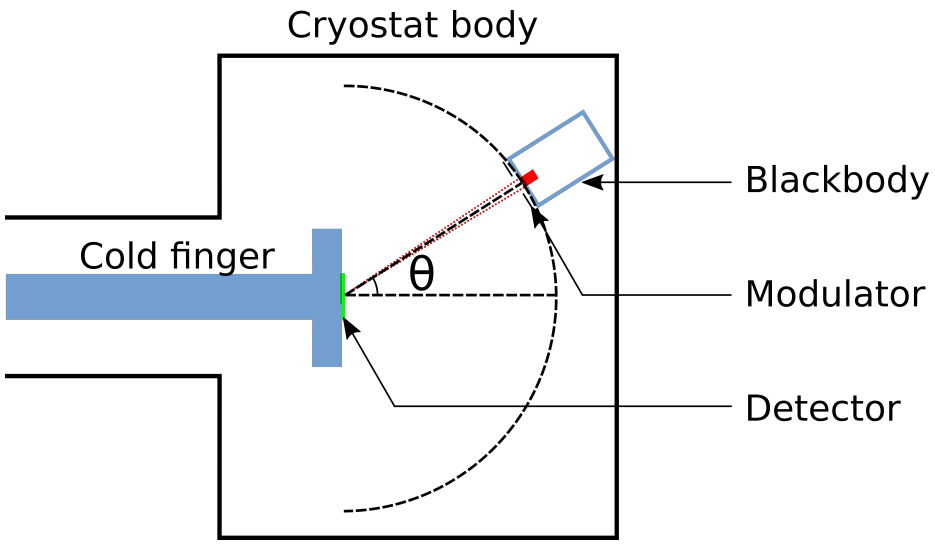

Figure 6. Schematic of the specific angular response measurement bench.

ACKNOWLEDGMENTS

Research funded by ASTRID nanoELASTIR project ANR-19-ASTR-0003. This work was partially funded by the French "Investment for the Future" program (EquipEx EXTRA, ANR-11-EQPX-0016).

REFERENCES

[1] Rehm, R., Lemke, F., Schmitz, J., Wauro, M., and Walther, M., "Limiting dark current mechanisms in antimony-based superlattice infrared detectors for the long-wavelength infrared regime," 94510N (June 2015).

[2] Klipstein, P., ""XB n " barrier photodetectors for high sensitivity and high operating temperature infrared sensors," 69402U (Apr. 2008).

[3] Martyniuk, P., Antoszewski, J., Martyniuk, M., Faraone, L., and Rogalski, A., "New concepts in infrared photodetector designs," *Applied Physics Reviews* **1**, 041102 (Dec. 2014). Number: 4.

[4] Massiot, I., Vandamme, N., Bardou, N., Dupuis, C., Lemaître, A., Guillemoles, J.-F., and Collin, S., "Metal Nanogrid for Broadband Multiresonant Light-Harvesting in Ultrathin GaAs Layers," *ACS Photonics* **1**, 878–884 (Sept. 2014). Number: 9.

[5] Chu, A., Gréboval, C., Goubet, N., Martinez, B., Livache, C., Qu, J., Rastogi, P., Bresciani, F. A., Prado, Y., Suffit, S., Ithurria, S., Vincent, G., and Lhuillier, E., "Near Unity Absorption in Nanocrystal Based Short Wave Infrared Photodetectors Using Guided Mode Resonators," *ACS Photonics* **6**, 2553–2561 (Oct. 2019). Number: 10.

[6] Taliercio, T. and Biagioni, P., "Semiconductor infrared plasmonics," *Nanophotonics* **8**, 949–990 (June 2019). Number: 6.

[7] Nordin, L., Kamboj, A., Petluru, P., Shaner, E., and Wasserman, D., "All-Epitaxial Integration of Long-Wavelength Infrared Plasmonic Materials and Detectors for Enhanced Responsivity," *ACS Photonics* **7**, 1950–1956 (Aug. 2020). Number: 8.

[8] Kamboj, A., Nordin, L., Petluru, P., Muhowski, A. J., Woolf, D. N., and Wasserman, D., "All-epitaxial guided-mode resonance mid-wave infrared detectors," *Applied Physics Letters* **118**, 201102 (May 2021).

[9] Maës, C., Vincent, G., Flores, F. G.-P., Cerutti, L., Haïdar, R., and Taliercio, T., "Infrared spectral filter based on all-semiconductor guided-mode resonance," *Optics Letters* **44**, 3090 (June 2019). Number: 12.

[10] Taliercio, T., Guilengui, V. N., Cerutti, L., Tournié, E., and Greffet, J.-J., "Brewster "mode" in highly doped semiconductor layers: an all-optical technique to monitor doping concentration," *Optics Express* **22**, 24294 (Oct. 2014). Number: 20.

[11] Hugonin, J. P. and Lalanne, P., "Reticolo software for grating analysis," (2005).

[12] Nguyen, B.-M., Hoffman, D., Wei, Y., Delaunay, P.-Y., Hood, A., and Razeghi, M., "Very high quantum efficiency in type-II InAs/GaSb superlattice photodiode with cutoff of 12 μm," *Applied Physics Letters* **90**, 231108 (June 2007). Number: 23.